J. Plasma Phys. (2022), *vol.* 88, 905880116
Published by Cambridge University Press

doi:10.1017/S0022377822000113

Global nature of magnetic reconnection during sawtooth crash in ASDEX Upgrade

O. Samoylov[1,†], **V. Igochine**[1], **A. Stegmeir**[1], **H. Zohm**[1] **and The ASDEX Upgrade Team**[1]

[1]Max Planck Institute for Plasma Physics, Boltzmannstr. 2, 85748 Garching, Germany

(Received 6 July 2021; revised 2 February 2022; accepted 3 February 2022)

This paper discusses the toroidal localisation of magnetic reconnection during sawtooth crashes. Numerical analysis with realistic heat diffusion coefficients shows that heat distributes itself helically along the torus faster than the temporal resolution of any existing ECE diagnostics. It makes local and global (helically axisymmetric) magnetic reconnection indistinguishable for an observer, while a local crash where the heat stays confined within a finite helical region could be distinguished. Statistical analysis of sawtooth crashes with the ECEI diagnostic is conducted in ASDEX Upgrade. The displacement of the heat within a finite helical region has not been observed. The statistical data supports global magnetic reconnection.

Key words: fusion plasma, plasma instabilities, plasma dynamics

1. Introduction

Sawtooth oscillations are internal periodic relaxation events in a tokamak that lead to a rapid redistribution of core temperature and density. The phenomenon of sawtooth oscillations has been known for decades, leading to the establishment of an extensive knowledge base for the prediction and control of the instability (Igochine *et al.* 2015). However, a conclusive theory that explains all the experimental observations of sawtooth oscillations has not yet been proposed and further investigations are required to fill the gaps in knowledge. The instability is expected to occur (i.e. is accepted in the operational procedure) in large fusion devices of the future such as ITER (Hu, Betti & Manickam 2006). Even though the temperature and density modulation due to sawteeth are predicted to have a moderate effect on both the plasma stored energy and the neutron production in ITER (Hender *et al.* 2007), the instability cannot be ignored. Sawteeth may seed neoclassical tearing modes (NTMs) (Chapman *et al.* 2010), which may lead to substantial loss of plasma energy and confinement degradation. Furthermore, NTMs may cause plasma disruptions (Zohm 2015) (sudden loss of plasma temperature and confinement). It is crucial to avoid plasma disruptions in future burning plasma machines because a plasma disruption is predicted to destroy the wall components. On the other hand, sawteeth could have a positive contribution to the transport of impurities (as well as helium ash in the future burning plasmas) from the core to the outer regions (Nave *et al.* 2003), in which case

† Email address for correspondence: oleg.samoylov@ipp.mpg.de

the controlled pacing of crashes would be beneficial for the operation. As the control and prediction of sawteeth are based on the sawtooth theory, the removal of knowledge gaps would result in better simulation and improved performance and safety of the machine operation. Apart from that, sawtooth crash requires magnetic reconnection, which is a phenomenon that is observed not only in laboratories but also in space plasmas (such as in solar flares, coronal mass ejection and the interaction of solar winds with the Earth's magnetosphere). Magnetic reconnection, by itself, is a subject of active research (Yamada, Kulsrud & Ji 2010). It is generally agreed that magnetic reconnection in laboratories has the same physical nature as magnetic reconnection in space (Yamada *et al.* 2010). Therefore, magnetic reconnection during sawtooth crashes can be used for testing existing theories against the observation.

One of the open questions is whether magnetic reconnection during the crash has global (everywhere along the $q = 1$ helical magnetic line) or local (only at a particular location on the $q = 1$ helical magnetic line) nature. Although most of the research published on sawtooth instability assumes that the crash occurs globally, there are multiple publications that report an observation of helical localisation of the crash (Nagayama *et al.* 1996; Munsat *et al.* 2007; Park 2019). The latter is the focus of our study. In § 2, we introduce existing models of the crash phase. In § 3, we present a numerical simulation of the heat redistribution during the crash. In § 4, we show our statistical study of sawtooth crashes in ASDEX Upgrade with ECEI diagnostic.

2. Existing models

The sawtooth oscillations cycle is described as follows. The temperature profile is relatively flat in the beginning of the cycle, and the safety factor value on the magnetic axis is above unity ($q(0) > 1$), as required for ideal stability. The plasma is heated ohmically (i.e. by collisions that resist the plasma current). As the current density is peaked on axis, the core of the plasma is preferentially heated, causing the temperature to peak in the core. As the resistivity decreases with increasing temperature ($\eta \propto T^{-3/2}$ for collisional plasma), the core becomes a relatively better electrical conductor than the edge, and the current density further peaks at $r = 0$, causing $q(0)$ to decrease. This leads to a further increase in the local heating rate, a further peaking of the temperature, and a further decrease in $q(0)$. When $q(0)$ value drops below unity, a $q = 1$ magnetic surface forms in the plasma core. In the vicinity of the $q = 1$ surface, the internal kink instability with poloidal mode number $m = 1$ and toroidal mode number $n = 1$ (or (1, 1) mode) is triggered. The (1, 1) kink mode is often called a precursor mode. Its nonlinear evolution leads to a crash: a rearrangement of the magnetic flux (magnetic reconnection) and flattening of the plasma temperature. The temperature inside the $q = 1$ surface exhibits a rapid decrease, whereas outside that surface it exhibits a rapid increase until the original state with relatively flat temperature and $q(0) > 1$ is restored. The cycle then repeats itself.

During a sawtooth crash, it is observed that the hot plasma core ($q \leq 1$) rapidly expels into the outer layers ($q > 1$). At the same time, it is still unclear whether the crash is helically axisymmetric (global, everywhere along the $q = 1$ helical line) or helically localised (local, in a particular place at the $q = 1$ line). A graphical representation of these two options is shown in figure 1.

Most of the sawtooth research to date assumes global reconnection. However, there are experimental reports (Nagayama *et al.* 1996; Munsat *et al.* 2007; Park 2019) that indicate the local reconnection during the crash. The ballooning effect (Park *et al.* 1995) and secondary instabilities (Bussac *et al.* 1984; Bussac & Pellat 1987; Gimblett & Hastie 1994) were suggested (Munsat *et al.* 2007) as a cause of the local reconnection.

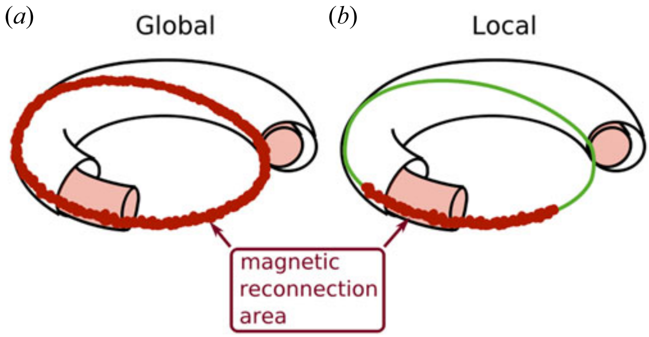

FIGURE 1. An artistic representation of the difference between global and local sawtooth crash. The global crash is shown in (*a*), where magnetic reconnection occurs everywhere along the $q = 1$ magnetic line. The local crash is shown in (*b*), where magnetic reconnection occurs only on a particular local place along the $q = 1$ magnetic line.

The following are existing theoretical sawtooth models with their dimensional descriptions of the phenomenon.

- Kadomtsev (Kadomtsev 1975): 2D ('2D' denotes a plasma model that has a two-dimensional poloidal and axisymmetric toroidal description; '3D' denotes a plasma model that is described with three-dimensional geometry), global.
- Ballooning (Bussac & Pellat 1987; Park *et al.* 1995): 3D, global and local are possible.
- Quasi-interchange:
  - Wesson (Wesson & Campbell 2011): 2D, global;
  - Jardin (Jardin, Krebs & Ferraro 2020): 3D, global.
- Stochastic (Lichtenberg *et al.* 1992; Igochine *et al.* 2006, 2008; Yu, Günter & Lackner 2015): 3D, global.

To simulate a sawtooth crash numerically, one needs to use two-fluid, nonlinear magnetohydrodynamic (MHD) codes in 3D geometry, which is a numerically expensive task. To reduce the numerical load it is a common approach to neglect the contribution of high toroidal mode numbers, which makes the reconnection global. The authors are aware of only three numerical studies on the ballooning effect influence on sawtooth crash with an assumption of the local magnetic reconnection: Baty, Luciani & Bussac (1992) (one-fluid MHD), Park *et al.* (1995) (MH3D code (Park *et al.* 1992), one-fluid MHD) and (Nishimura, Callen & Hegna 1999) (one-fluid MHD, heat conduction parallel to the magnetic field is ignored). The authors are not aware of any recent numerical studies that simulate helically local magnetic reconnection during a sawtooth crash and include all important physical effects (two-fluid MHD, nonlinear, plasma resistivity, high toroidal mode number, realistic Lundquist number $S > 10^7$).

3. Heat distribution

During a sawtooth crash, there is an opening through which magnetic lines from the plasma core ($q < 1$) reconnect with magnetic lines in the outer plasma layers ($q > 1$) (shown in red in figure 1). The hotter core plasma mixes with colder plasma in the outer layers through this opening to form a 'heat bridge'. In this section, we model the heat redistribution during the crash.

https://doi.org/10.1017/S0022377822000113 Published online by Cambridge University Press

To simulate the heat redistribution during a sawtooth crash, we used the GRILLIX code (Stegmeir *et al.* 2018). The GRILLIX code is able to solve the heat diffusion equation in axisymmetric cylindrical geometry with a constant-in-time magnetic field profile:

$$\frac{\mathrm{d}T}{\mathrm{d}t} = \chi_{\parallel}\nabla_{\parallel}^{2}T + \chi_{\perp}\nabla_{\perp}^{2}T. \tag{3.1}$$

We assume a local sawtooth crash with a three-dimensional Gaussian heat source along the $q = 1$ helical magnetic line (figure 2*a*). The source has the following dimensions (full width at half maximum): ≈ 5.8 cm in r_x and r_y coordinates (a typical size of X-point during sawtooth crash in ASDEX Upgrade), approximately 50° of toroidal angle along $q = 1$ magnetic line. The realistic plasma parameters and dimensions were used: tokamak major radius $R_0 = 1.65$ m, radius of $q = 1$ magnetic surface $r_{q=1} = 0.15$ m) as well as a realistic ratio of parallel and perpendicular heat transport coefficients $\chi_{\parallel}/\chi_{\perp} = 2 \times 10^{8}$ (estimated in Appendix A). The used q profile is shown in figure 2(*b*). The code is limited to a constant-in-time q profile, which is a good assumption for the initial phase of the heat redistribution. Thus, we are able to simulate the initial phase of the sawtooth crash when the reconnection just starts. As we show, this simulation is sufficient to make a conclusion about the heat redistribution at the first stage of the crash.

In figure 2(*a*), we show two poloidal cross-sections of a tokamak (marked as 'A' and 'B'), which are located toroidally 180° apart. We observe both cross-sections during our simulation: in 'A' we locate the centre of the heat source, whereas in 'B' we observe the speed and manner of the heat redistribution. The result of this simulation is shown in figure 2(*c*). The helically localised heat source redistributes itself in a helically symmetric manner during approximately 100 ns time due to the high heat conductivity of electrons along the magnetic field lines. Variation of the safety factor profile from $q_0 = 0.6$ (high magnetic shear) to $q_0 = 0.999$ (low magnetic shear) does not change the result. The result is also robust with respect to the toroidal extent of the localised reconnection zone along the $q = 1$ line (heat source in figure 2*a*). Even in the case of a narrow 'single point' reconnection width, the result remains the same.

As we mentioned earlier, the GRILLIX simulation of the heat distribution assumes a constant magnetic field, which is not the case during a sawtooth crash. However, the time scales of the heat distribution ($\tau_{\text{heat distr.}} \approx 0.1\ \mu\text{s}$) and the crash ($\tau_{\text{crash}} \approx 100\ \mu\text{s}$ in ASDEX Upgrade) differ dramatically ($\tau_{\text{crash}}/\tau_{\text{heat distr.}} = 1000$). This means that magnetic reconnection during the crash is practically a static process compared with the heat distribution. In other words, the electron temperature on slowly reconnected field lines would be almost immediately equilibrated. This rationale justifies the assumption of a constant magnetic field made in the GRILLIX.

In present-day tokamaks, there is no diagnostic tool for core MHD activity with sufficient temporal resolution to trace the process of heat equilibration at a nanosecond scale. To observe the localised heat redistribution, one needs to have a diagnostic with a temporal resolution in the order of tens of nanoseconds. However, the fastest temporal resolution currently available is approximately 1 μs (in the current paper, the temporal resolution of the used diagnostic has been increased to 5 μs in order to reduce the signal noise). As a result, we cannot distinguish between a global and a local magnetic reconnection experimentally, which is the main conclusion from our GRILLIX simulation. Our current diagnostics would detect global heat redistribution (figure 1*a*) even when the magnetic reconnection is local (figure 1*b*).

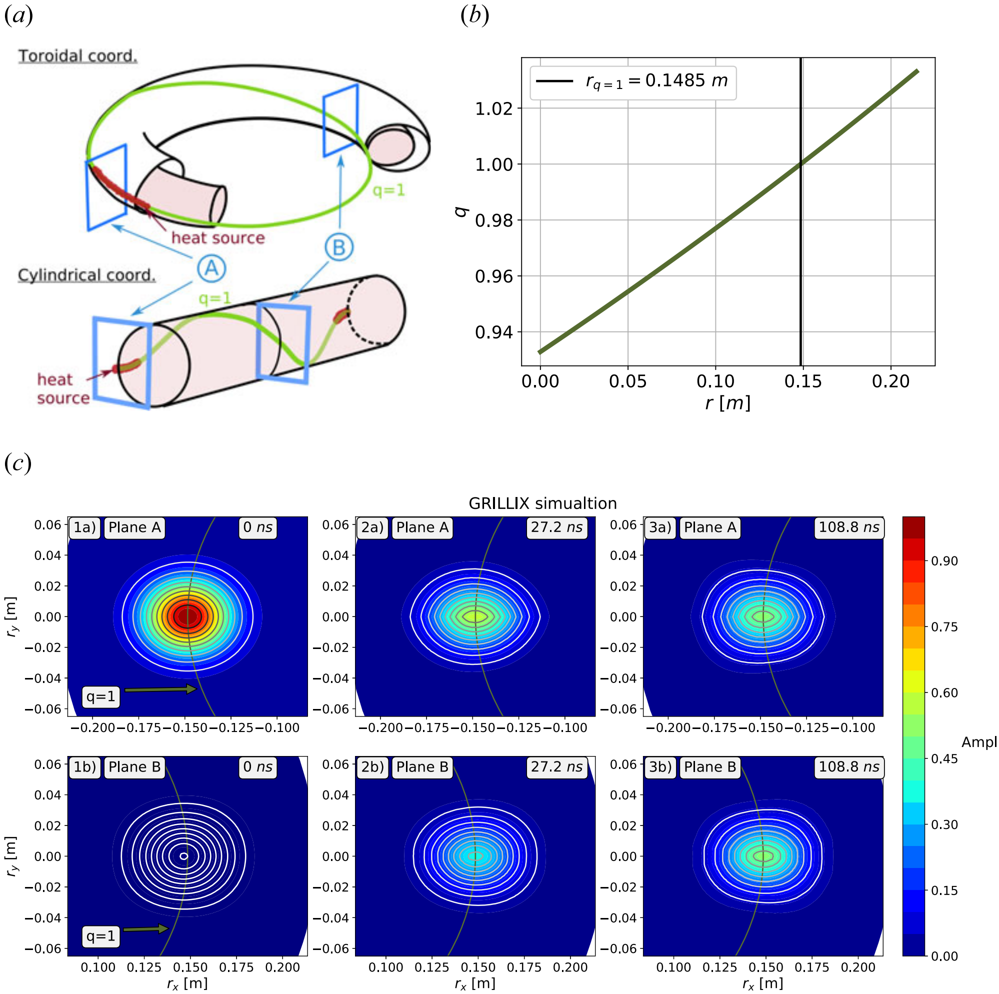

FIGURE 2. Simulation of heat distribution at the beginning of a sawtooth crash with GRILLIX. In (*a*), an artistic representation of the geometry is shown. The observed planes (planes 'A' and 'B') are located toroidally 180° apart with the heat source localised in one of them. In (*b*), the used safety factor q profile is shown. In (*c*), the result of the simulation is shown.

4. Statistical analysis of sawtooth crashes

The previous section showed that the helically symmetric heat distribution along the torus is on a faster time scale than is accessible by the state-of-the-art diagnostics for tokamaks. For that reason, we concluded that we are unable to distinguish between local and global reconnection as long as the local reconnection leads to an outflow of heat to (initially) unperturbed field lines just outside $q = 1$. However, another group (Munsat *et al.* 2007) has reported experimental evidence of the helically (i.e. both toroidally and poloidally) localised sawtooth crash observation, contradicting our initial conclusion. Munsat *et al.* (2007) stated that there is no clear physical understanding of the local crash phenomenon. They refer to a hybrid ballooning mode and/or effect of a secondary instability as a possible cause. We interpret the reported local crash observation as a radial displacement of the hot core plasma region, which is observed by ECEI and inferred

https://doi.org/10.1017/S0022377822000113 Published online by Cambridge University Press

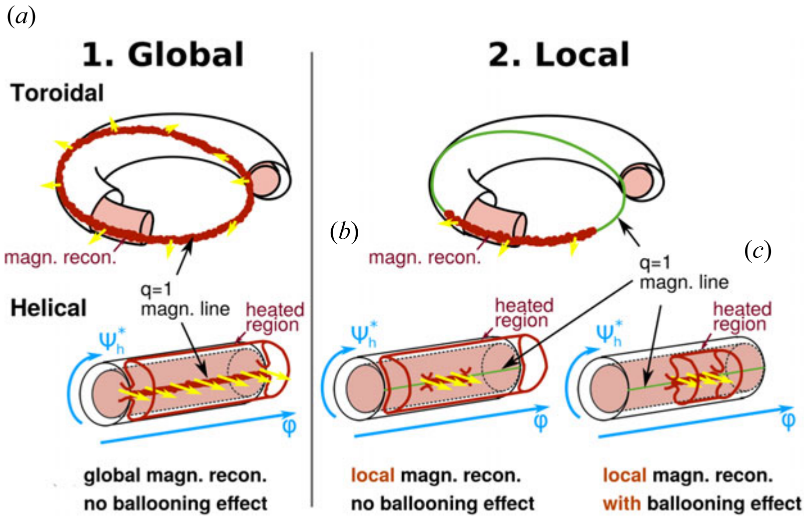

FIGURE 3. Artistic representation of the considered sawtooth crashes: (*a*) global magnetic reconnection without ballooning effect, (*b*) local magnetic reconnection without ballooning effect and (*c*) with ballooning effect (some plasma fluxes are displaced to the area outside $q = 1$ magnetic surface prior to the local magnetic reconnection). The helical coordinates are used to clearly show the difference between the three cases.

as local magnetic reconnection. The explanation would require an unknown helically localised magnetic confinement structure during the crash that we have not modelled with GRILLIX. This leads us to two cases of local magnetic reconnection. To clearly distinguish between these cases, we introduce an artistic representation of the magnetic reconnection in helical coordinates in figure 3, where three cases are shown:

(i) global magnetic reconnection without ballooning effect, shown in figure 3(*a*);
(ii) local magnetic reconnection without ballooning effect (case observed in GRILLIX simulation in the previous section), shown in figure 3(*b*)'
(iii) local magnetic reconnection with ballooning effect, where some plasma fluxes are displaced to the area outside $q = 1$ magnetic surface in a helically confined region (case possibly observed by Munsat *et al.* 2007), shown in figure 3(*c*).

We assume the local displacement of plasma fluxes outside $q = 1$ magnetic surface in a helically confined region (figure 3*c*) as given hypothesis. In this section, we use the term ‘local sawtooth crash’ with reference to the hypothesis. The cases (*a*) and (*b*) in figure 3 are indistinguishable for our diagnostic and observed as ‘global’ crash. To test this hypothesis, we checked whether we can experimentally observe the described local sawtooth crash in ASDEX Upgrade.

Ideally, one would need to compare the observations from several diagnostics at different tokamak toroidal angles (different poloidal cross-sections of the tokamak) to experimentally distinguish between global and local sawtooth crashes. On ASDEX Upgrade, there are four diagnostics that may be used to study core MHD activity: ECE, ECEI, SXR and Mirnov coils (for a description of these diagnostics and their usages to study MHD modes, please refer to Igochine *et al.* (2015); and for a more thorough overview of ECEI, refer to Tobias *et al.* (2009) and Classen *et al.* (2010)). It is not possible to determine the localisation of the crash with Mirnov coils. Although the SXR diagnostic

https://doi.org/10.1017/S0022377822000113 Published online by Cambridge University Press

has been shown to be good for studying the pre-crash phase of sawtooth instability (Vezinet *et al.* 2016) and has a toroidal separation by approximately 45° from the ECE diagnostic (ECE and ECEI are located at the same poloidal plane), it does not have a sufficient number of lines of sight to resolve the crash phase. Thus, the SXR diagnostic cannot be combined with ECEI to distinguish local and global crashes.

Another approach to the problem is using statistical analysis. Namely, we can count how many times we see the crash in the ECEI window for a certain (1, 1) mode rotation frequency. Thus, we can estimate the probability of a sawtooth crash observation in the ECEI window for a certain (1, 1) mode frequency. For different (1, 1) mode frequencies, we can then plot the dependence of the observation probability on the frequency of the mode. This dependence will look different for local and global sawtooth crashes, as the observation probability of the global crash will be higher than the probability of the local one. The dynamics of sawtooth crash in ASDEX Upgrade can be studied thanks to the sufficient temporal ($\Delta t_{ECEI} = 5\ \mu s$) and spatial two-dimensional (12 by 40 cm, 8 by 16 channels) resolutions of the ECEI diagnostic. Examples of two sawtooth crashes measured in ASDEX Upgrade, one inside and one outside of the ECEI window, are shown in figure 4. A similar statistical approach has been applied by Munsat *et al.* (2007) in TEXTOR tokamak, where the authors analysed 47 sawtooth crashes but all with the same rotation mode frequency. Under the assumption that the toroidal and poloidal centre of the localised reconnection zone occurs at a random location on the $q = 1$ surface, the authors estimated the probability of the crash occurring within the ECEI observation window as

$$P_{\text{obs in ECEI}} = \frac{\Delta\theta_{\text{ECEI}} + \Delta\theta_{\text{rec}} + \Delta\phi_{\text{rec}}}{2\pi}, \tag{4.1}$$

where $\Delta\theta_{\text{ECEI}}$ is the poloidal coverage of the ECEI window, and $\Delta\theta_{\text{rec}}$ and $\Delta\phi_{\text{rec}}$ are the poloidal and toroidal angles, respectively, of the reconnection zone. Taking the $P_{\text{obs in ECEI}}$, $\Delta\theta_{\text{ECEI}}$, $\Delta\theta_{\text{rec}}$ from the experimental data ($P_{\text{obs in ECEI}} \approx 50\,\%$, $\Delta\theta_{\text{ECEI}} \approx 60^\circ$, $4^\circ \lesssim \Delta\theta_{\text{rec}} \lesssim 14^\circ$), the authors estimated the toroidal angle of reconnection zone localisation to be $\Delta\phi_{\text{rec}} \approx 108^\circ$–$126^\circ$.

In the ASDEX Upgrade tokamak we:

(i) reproduced the observation of TEXTOR by measuring the same experimental parameters ($P_{\text{obs in ECEI}}$, $\Delta\theta_{\text{ECEI}}$, $\Delta\theta_{\text{rec}}$);

(ii) expanded the study by analysing sawtooth crashes at different mode frequencies (in TEXTOR, the crashes were analysed only at a single frequency); thus, we can determine the experimental dependency of the crash observation on the mode frequency $P_{\text{obs in ECEI}}(\nu_{\text{mode}})$ and compare it with the theoretical prediction for local and global crashes.

To understand whether we can use (4.1) to theoretically estimate $P_{\text{obs in ECEI}}(\nu_{\text{mode}})$ in ASDEX Upgrade, we first discuss its applicability. Equation (4.1) is derived for sawtooth crashes that have a duration of at least one toroidal turn of the mode. In both tokamaks, ASDEX Upgrade and TEXTOR, it is challenging to experimentally determine the precise crash duration due to the influence of the (1, 1) mode rotation on the measured signal, the nonlinear character of the phenomenon and the limited toroidal coverage of available plasma diagnostics. In the best-case scenario, one can determine the upper limit of the crash duration. The sawtooth crashes analysed in Munsat *et al.* (2007) had a (1, 1) mode frequency of $f_{\text{mode}} = 6.5$ kHz. As the authors assumed that the crash evolves linearly on the timescale of one toroidal turn, the crash duration was assumed to be $t_{\text{crash}} = 1/f_{\text{mode}} \approx 150\ \mu s$.

(*a*)

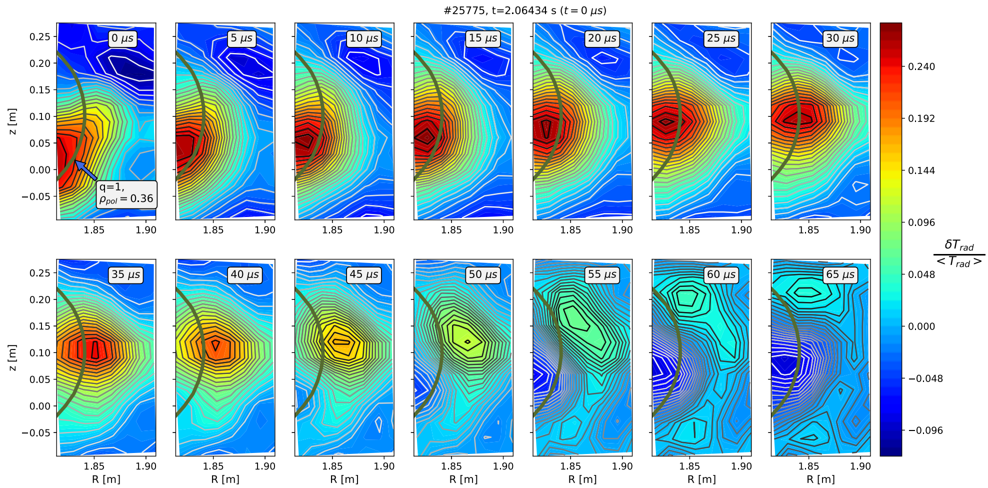

(*b*)

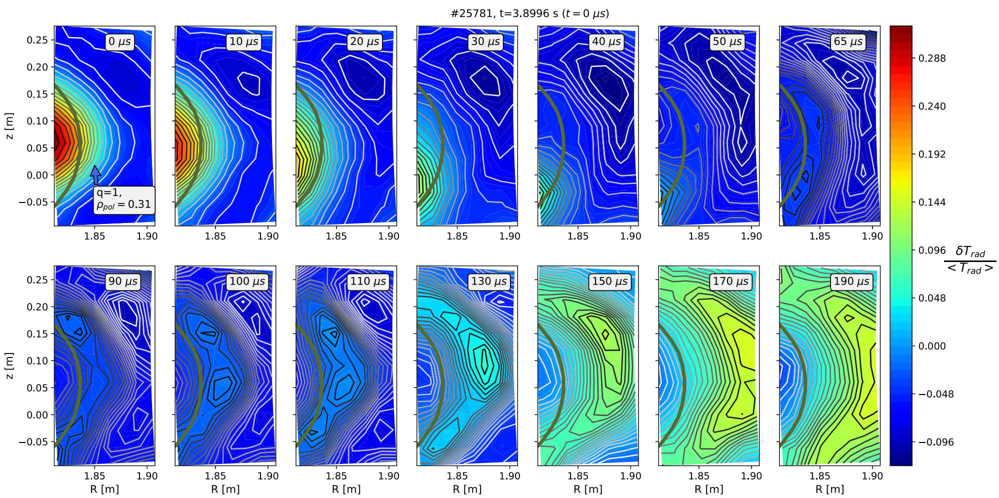

FIGURE 4. Examples of two sawtooth crashes measured with the ECEI diagnostic in ASDEX Upgrade: (*a*) inside and (*b*) outside of the ECEI window. Here $\delta T_{\mathrm{rad}}/\langle T_{\mathrm{rad}}\rangle$ is normalised fluctuation of electron radiation temperature, and R and z correspond to the major radius and vertical axis of the tokamak, respectively.

Our experimental database of sawtooth crashes in ASDEX Upgrade has (1, 1) mode frequencies in a range of 0.5 to 11.5 kHz. The frequency of the (1, 1) mode and the velocity of toroidal plasma rotation are mainly determined by the NBI sources (the values for different shots are listed in table 2 of Appendix B). All crashes in the database have a crash time duration of less than one toroidal turn of the plasma. We estimate the upper limit of the crash time from the shortest mode period that is available in the database: $t_{\mathrm{crash}}^{\mathrm{ASDEX}} \leq 1/\max(f_{\mathrm{mode}}) \approx 90\ \mu\mathrm{s}$. Therefore, (4.1) is not applicable for most of our data (it is marginally applicable only for the highest mode frequency).

To estimate $P_{\mathrm{obs\ in\ ECEI}}(f_{\mathrm{mode}})$ for the whole frequency range, we instead build a numerical model that simulates the observation of a sawtooth crash by ECEI. The position

https://doi.org/10.1017/S0022377822000113 Published online by Cambridge University Press

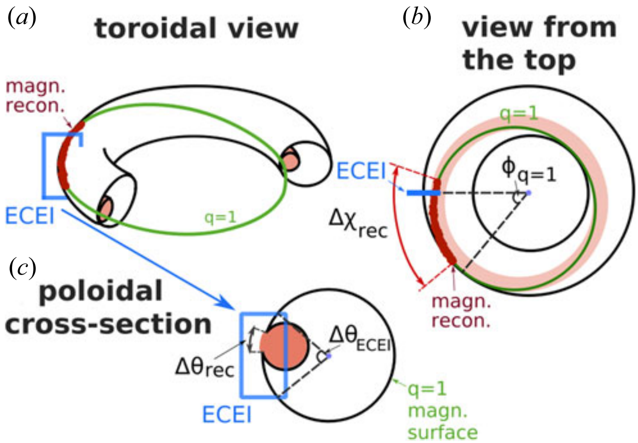

FIGURE 5. Artistic representation of the statistical model of sawtooth crash from (*a*) toroidal 3D, (*b*) top and (*c*) poloidal cross-section views. The magnetic reconnection size is described with toroidal $\Delta\chi_{rec}$ and poloidal $\Delta\theta_{rec}$ angles. Here $\phi_{q=1}$ is the toroidal angle between the lowest field side of the mode and the ECEI plane at the beginning of the model run and $\Delta\theta_{ECEI}$ is the poloidal coverage of the $q = 1$ magnetic surface.

of the magnetic reconnection should be randomly set for each run of the model. Then, by running the model multiple times, one receives the statistical observation for a given (1, 1) mode frequency, poloidal/toroidal angles of the reconnection zone, and ECEI window size.

Our statistical model provides a two-dimensional description of a sawtooth crash (figure 5*b*). It describes the magnetic reconnection of the crash as an opening in the $q = 1$ magnetic line (red region in figure 5) through which the hot plasma core expels to the outer magnetic surfaces ($q > 1$). The opening size is described by the toroidal angle $\Delta\chi_{rec}$ and poloidal angle $\Delta\theta_{rec}$ (figure 5*b* and 5*c*). Here $\Delta\chi_{rec} = 120^\circ$ is taken from Munsat *et al.* (2007), which is the only experimentally reported toroidal angle value of the local sawtooth crash known to us. We evaluate $\Delta\theta_{rec}$ from the 2D temperature profiles received from the ECEI. The angle corresponds to the size of the opening in the $q = 1$ magnetic surface through which heat expels from the core to the outer magnetic surfaces ($q > 1$). An example of this opening can be observed in figure 4(*a*), time frames 25–40 μs. The value $\Delta\theta_{rec} \approx 15^\circ$ is obtained as the average from several sawtooth crashes. The blue horizontal line represents the ECEI window coverage. It covers the poloidal angle $\Delta\theta_{ECEI} \approx 90^\circ$ (evaluated from the experimental data) of the $q = 1$ magnetic surface. The (1, 1) mode rotates relative to the ECEI window with a constant frequency f_{mode}. The time duration of one simulation run corresponds to the upper limit of the sawtooth crash duration, that we estimated earlier ($t_{crash}^{ASDEX} \approx 90$ μs). The time step of the model corresponds to the ECEI temporal resolution ($dt_{ECEI} = 5$ μs). If during the simulation run the red crash zone crosses the ECEI coverage (blue horizontal line), then the crash is observed by the ECEI diagnostic. At the start of each model run, for the local crash we set randomly: (*a*) the initial toroidal angle $\phi_{q=1}$ that is between the lowest field side of the mode and the ECEI plane; and (*b*) initial localisation of the magnetic reconnection centre on the $q = 1$ magnetic line. For the global crash, only the $\phi_{q=1}$ parameter is used, because $\Delta\chi_{rec} = 2\pi$. For each given mode frequency f_{mode} we make $N = 10^5$ simulation runs. We then count how many times we observe the crash in the ECEI window N_{obs}. Lastly, we receive the probability of observation from $P_{obs\ in\ ECEI}(f_{mode}) = N_{obs}/N$. For a summary of input parameters of the model, please refer to Appendix B.

https://doi.org/10.1017/S0022377822000113 Published online by Cambridge University Press

Our experimental statistics include data from 167 sawtooth crashes from 6 plasma discharges. For a summary of plasma parameters, please refer to Appendix B. The frequency of the (1, 1) mode is obtained from SXR and Mirnov coils diagnostics. In all the analysed sawtooth crashes, there is a post-cursor (a mode that exists after the crash or ‘survives’ the crash). Therefore, we have obtained data of the mode frequency from just before the crash (f^B_{mode}) and directly after the crash (f^E_{mode}). For the statistical analysis we took an average frequency value ($(f^B_{mode} + f^E_{mode})/2$). To note, for our data, the difference between f^B_{mode} and f^E_{mode} lays within 10 % and the choice of the mode frequency for the analysis (f^B_{mode}, f^E_{mode} or $(f^B_{mode} + f^E_{mode})/2$) did not significantly affect the final statistic or change the conclusions. Two digital filters were applied during the ECEI analysis for noise reduction: Savitzky–Golay (Schafer 2011) and 2D Gaussian (Scipy-ndimage 2020). Figure 4 displays the data after application of these two filters.

The comparison between the experimental and the numerically predicted $P_{\text{obs in ECEI}}$ (f_{mode}) is shown in figure 6. The error of the experimental data corresponds to the standard error of the Gaussian-type statistic (standard error = standard deviation $\sigma/\sqrt{\text{sample } n \text{ observations}}$). As discussed earlier, (4.1) is marginally applicable only for the highest (1, 1) mode frequency of 11 kHz. The calculated statistic for this frequency is shown by the red column. The result from Munsat *et al.* (2007) is shown by the black column, although it is beyond the applicability of (4.1) because in ASDEX Upgrade the duration of the crash is faster than one toroidal turn of the mode. The red and black columns have the same probability, because (4.1) does not consider the rotation frequency of the (1, 1) mode. Local and global results from the numerical simulation are shown by the yellow and blue columns, respectively. Overall, our experimental statistic fits the global model better over the whole frequency range, except for the 3.5–4.5 kHz. This discrepancy is likely due to an insufficient statistical number of observations for this frequency range. The used crash duration of 90 μs is the upper limit in ASDEX Upgrade. With a lower value of the crash duration, the probability of the crash observation decreases for both local and global crashes. Therefore, shorter crash duration enlarges the statistical distinction between experimental results and the local statistic (figure 6), and makes the global crash model resemble the experimental observation even more.

To summarise, local sawtooth crash (localised displacement of plasma fluxes outside the $q = 1$ magnetic surface (figure 3*c*) was not observed in ASDEX Upgrade. The observation of a local crash in TEXTOR (Munsat *et al.* 2007) has been done for a single frequency of the (1, 1) mode (6.5 kHz). It is difficult to draw a conclusion between the local and global crashes from this single point as one can see in figure 6. The comparison across several frequencies leads to a more robust conclusion than with a single frequency. We observe only global (figure 3*a*) or local (figure 3*b*) magnetic reconnection scenarios, which, as we discussed in the previous section, are indistinguishable from each other for the current state-of-the-art tokamak diagnostic due to insufficient temporal resolution. The numerical simulations show that with reduction of $\Delta\chi_{rec}$ (figure 5*b*), the difference in probability of the crash observation by ECEI grows between global and local cases. An increase of $\Delta\chi_{rec}$ leads to a smaller difference between the global and local cases. The difference vanishes at $\Delta\chi_{rec} = 360^\circ$.

5. Conclusion

In this paper, we have studied the helical localisation of magnetic reconnection during sawtooth crashes in ASDEX Upgrade. Most research conducted on sawteeth to date either considered that a sawtooth crash has 2D nature (helically symmetric) or have not addressed the question of possible helical asymmetry. However, there are numerical (Park *et al.* 1995;

https://doi.org/10.1017/S0022377822000113 Published online by Cambridge University Press

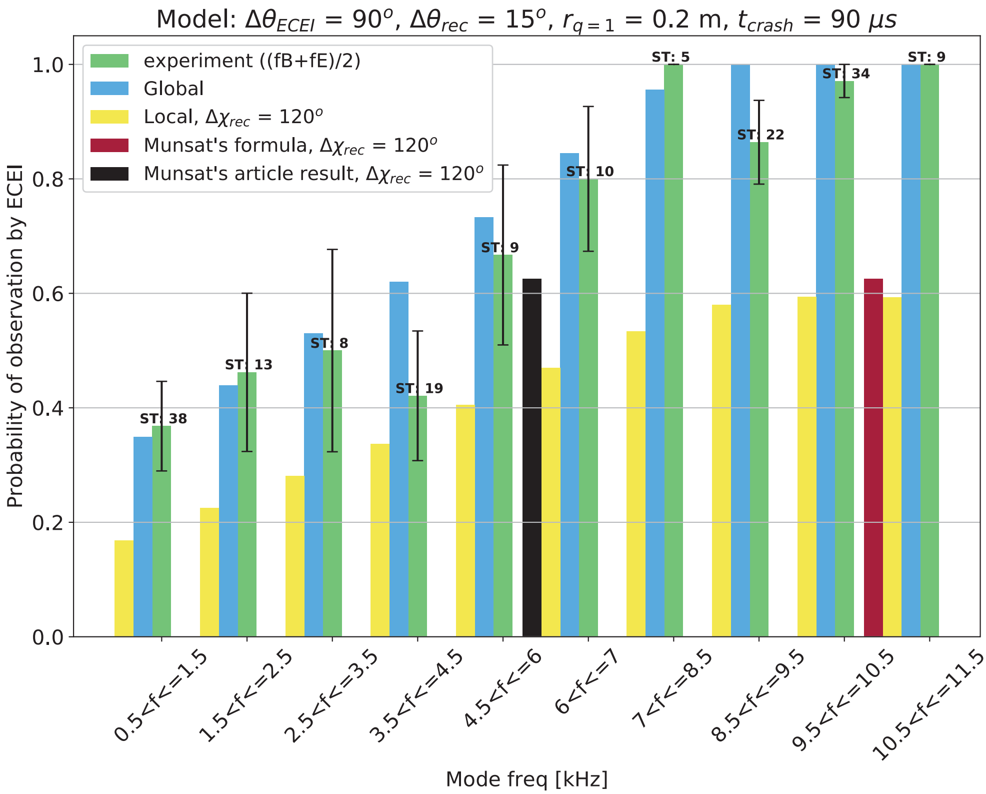

FIGURE 6. Probability of sawtooth crash observation in the ECEI window with the dependence on the (1, 1) mode frequency $P_{\text{obs in ECEI}}(f_{\text{mode}})$. In green are the experimental measurements in ASDEX Upgrade. The results from the global and local crash statistical model are shown in blue and yellow colours, respectively. The result calculated with (4.1) is shown: (*a*) in red for the frequencies where the equation is valid; (*b*) in black for the frequency used in Munsat *et al.* (2007).

Nishimura *et al.* 1999) and experimental (Nagayama *et al.* 1996; Munsat *et al.* 2007) works with a sawtooth crash helically localised in the toroidal plane.

First, we numerically studied the possibility of an experimental measurement for the helical localisation of the magnetic reconnection. We have modelled the heat propagation at the initial stage of sawtooth crash with the GRILLIX code (Stegmeir *et al.* 2018) using experimental plasma parameters. The result of this modelling has shown that the heat redistributes helically along the torus on a much faster time scale (0.1µs) than is accessible by the state-of-the-art diagnostics of tokamaks (currently, the minimal accessible value is 1 µs; in this paper, the temporal resolution of 5 µs is used in order to reduce the signal noise). Thus, one cannot distinguish between the global and local magnetic reconnection experimentally, because of the extremely fast redistribution of the heat along the magnetic field lines.

Second, we investigated experimental evidence of local magnetic reconnection reported in TEXTOR (Munsat *et al.* 2007). Munsat *et al.* (2007) conducted a statistical analysis of Sawtooth crashes with ECEI diagnostic. Their analysis assumes a toroidally localised heat distribution during the crash. We took the hypothesis as given and conducted a statistical analysis of crashes in ASDEX Upgrade with ECEI diagnostic for a broad

https://doi.org/10.1017/S0022377822000113 Published online by Cambridge University Press

range of (1, 1) mode frequencies (0.5–11.5 kHz). Our analysis showed good agreement with the global sawtooth crash scenario and did not reveal evidence for the local heat redistribution. Observations in TEXTOR were conducted with a singular (1, 1) mode frequency (6.5 kHz) and the analysis was done with an assumption that crash has a time duration of one toroidal turn of the mode. Due to these two factors, it is hard to distinguish between local and global crashes (see figure 6, the data for the mode frequencies from 6 to 7 kHz) in the measurements conducted by Munsat *et al.* (2007).

We conclude that even though one cannot exclude an event of local magnetic reconnection and the resulting fast redistribution of heat along the field lines, these events will be indistinguishable from global reconnection in all present-day ECE diagnostics.

Acknowledgements

We are grateful to A. Gude, M. Willensdorfer and W. Suttrop for their critical questions, which have given us alternative perspectives on our research. We thank B. Vanovac for sharing her technical knowledge of the ECEI diagnostic and experience in the analysis of ECEI data with us. We thank Q. Yu for sharing his extensive knowledge in physics and numerical simulation of sawtooth crash. Finally, we thank M.J. Choi for sharing their analysis methods of ECEI data that are commonly used in KSTAR tokamak.

Editor Troy Carter thanks the referees for their advice in evaluating this article.

Declaration of interests

The authors report no conflict of interest.

Funding

This work has been carried out within the framework of the EUROfusion Consortium and has received funding from the Euratom research and training programme 2014–2018 and 2019–2020 under grant agreement No. 633053. The views and opinions expressed herein do not necessarily reflect those of the European Commission.

Data availability statement

The data that supports the findings of this study are available from the corresponding author upon reasonable request.

Appendix A. Transport coefficients in GRILLIX

In collisionless plasma, as in the core plasma of ASDEX Upgrade, parallel transport coefficient $\chi_{\parallel}$ can be estimated with (Chang & Callen 1992):

$$\chi_{\parallel} = \frac{\chi_{\mathrm{SH}}}{\sqrt{1 + \left(3.16 \dfrac{v_{\mathrm{th},e}}{\nu_{\mathrm{ei}} L_c}\right)^2}} \left[\frac{\mathrm{m}^2}{\mathrm{s}}\right], \tag{A1}$$

where χ_{SH} is the classical Spitzer–Härm formula χ_{SH} (Spitzer & Härm 1953) for perpendicular transport coefficient in collisional plasma

$$\chi_{\mathrm{SH}} = 3.16 v_{\mathrm{th},e} \lambda_e = 3.6 \times 10^{29} \frac{Te[\mathrm{keV}]^{5/2}}{n_e[\mathrm{m}^{-3}]}\ \mathrm{m}^2\ \mathrm{s}^{-1}, \tag{A2}$$

Parameter	**Value**	**Description**
$r_{q=1}$	0.2 m	Radius of $q=1$ magn. surf
R_0	1.65 m	ASDEX Upgrade major radius
t_{crash}	90 μs	Time duration of sawtooth crash (duration of simulation)
dt_{ECEI}	5 μs	ECEI temporal resolution (simulation time step)
$\Delta\theta_{ECEI}$	90°	Poloidal coverage of $q=1$ magn. surf by ECEI window
f_{mode}	0.5–11.5 kHz, step 0.5 kHz	Frequency range of the (1, 1) mode
N	10^5	Number of simulation runs on a singular (1, 1) mode frequency f_{mode}
$\Delta\theta_{rec}$	15°	Poloidal angle of magnetic reconnection (taken from experimental data)
$\Delta\chi_{rec}$	120° for local crash 360° for global crash	Toroidal angle of magnetic reconnection (taken from Munsat *et al.* (2007) for local crash)
$\phi_{q=1}$	0–360°, set randomly at each model run	Initial toroidal angle between ECEI window and the lowest field side of $q=1$ magnetic line on which the magnetic reconnection occurs
χ_0	0–360°, set randomly at each model run for local crash (not relevant for global crash)	The initial localisation of magnetic reconnection centre on $q=1$ magnetic line

TABLE 1. Input parameters of the statistical model.

and ν_{ei} is the electron–ion collision frequency (Chen 2016, p. 415)

$$\nu_{ei} = 2\times 10^{-6}\frac{Zn_e[\mathrm{cm}^{-3}]\ln\Lambda}{T_e^{3/2}[\mathrm{eV}]}[\mathrm{s}^{-1}]. \tag{A3}$$

In these equations, $v_{th,e}$ is the electron thermal velocity, λ_e is the mean free path of electrons, T_e and n_e are the electron temperature and density, respectively, L_c is the heat connection length, Z is the ion charge state and $\ln\Lambda$ is the Coulomb logarithm.

The plasma parameters of the sawtooth crashes considered in this paper are: $Z=2$ (deuterium plasma), $T_e\approx 3$ keV, $n_e\approx 5\times 10^{19}$ m^{-3}, $\ln\Lambda=17$ and $L_c=2\pi R_0=10.4$ m (R_0 is major radius of ASDEX Upgrade). The results of the calculation are as follows: $v_{th,e}=2.3\times 10^7$ m s, $\nu_{ei}=10^4\mathrm{s}^{-1}$, $\chi_{SH}=1.1\times 10^{11}$ m^2 s^{-1} and $\chi_\parallel\approx 2\times 10^8$ m^2 s^{-1}.

The perpendicular heat transport coefficient is taken as a typical value for an ASDEX Upgrade discharge in the core plasma $\chi_\perp\approx 1\mathrm{m}^2$ s^{-1} (Luda *et al.* 2020). The ratio between parallel and perpendicular coefficients is $\chi_\parallel/\chi_\perp=2\times 10^8$. Such high anisotropies can be handled with GRILLIX thanks to the flux-coordinate-independent approach in combination with the support operator method (Stegmeir *et al.* 2016). In addition, the results in § 3 were found to be converged in resolution.

Appendix B. Parameters and values used

Input parameters of the statistical model are listed in table 1 (see figure 5 as a schematic representation of the listed parameters).

https://doi.org/10.1017/S0022377822000113 Published online by Cambridge University Press

Shot	t (s)	f_{mode} (kHz)	N_{ST}	I_p (MA)	NBI (MW)	ECRH (MW)	ICRH (MW)	n_e ($\times 10^{19}$ m^{-3})
25775	1.8–2.8	1.0–6.0	24	1	0–2.6	0	4.5	8.6
25781	2.1–5	0.5–10.0	54	1	2.6–5.2	0.8–1.7	4.5	8.8
25782	2.26–3.35	1.0–11.0	14	1	5.1	1.7	4.3	8.8
25783	2.07–2.46	1.2–9.5	9	1	5.1	0.7	3.7	9.6
25785	2.17–5.85	1.0–11.0	42	1	5.1	0	0–4.3	8.6
26333	1.41–1.97	3.0–7.5	7	0.7	5.2	0.7	0	6.5
26612	1.62–1.96	2.0–3.6	10	0.8	2.5	0	2.37	4.8
26717	1.57–1.93	6.0–10.0	7	1	2.5–5.0	0.8	0	9.5

TABLE 2. Plasma parameters of the analysed discharges.

Plasma parameters of the analysed discharges from § 4 are summarised in table 2. The following notation is used: t and f_{mode} are the time and mode frequency ranges, respectively, of the analysed sawteeth in a specific shot; I_p is the plasma current; NBI is the neutral beam injection; ECRH and ICRH are the electron and ion cyclotron resonant heating, respectively; and n_e is the average plasma density received from interferometry. The axial toroidal magnetic field for all considered shots was $B_t = 2.5$ T.

REFERENCES

BATY, H., LUCIANI, J.-F. & BUSSAC, M.-N. 1992 Asymmetric reconnection and stochasticity in tokamaks. *Nucl. Fusion* **32** (7), 1217–1223.

BUSSAC, M.N. & PELLAT, R. 1987 Nonlinear evolution of the internal kink in tokamaks. *Phys. Rev. Lett.* **59** (23), 2650–2653.

BUSSAC, M.N., PELLAT, R., SOULE, J.L. & TAGGER, M. 1984 Half-coalescence of the $m = 1, n = 1$ magnetic island in tokamaks. *Phys. Lett.* A **105** (1), 51–53.

CHANG, Z. & CALLEN, J.D. 1992 Unified fluid/kinetic description of plasma microinstabilities. Part II: applications. *Phys. Fluids* B **4** (5), 1182–1192.

CHAPMAN, I.T., *et al.* 2010 Empirical scaling of sawtooth period for onset of neoclassical tearing modes. *Nucl. Fusion* **50** (10), 102001.

CHEN, F.F. 2016 *Introduction to Plasma Physics and Controlled Fusion*. Springer.

CLASSEN, I.G.J., BOOM, J.E., SUTTROP, W., SCHMID, E., TOBIAS, B., DOMIER, C.W., LUHMANN, N.C., DONNÉ, A.J.H., JASPERS, R.J.E., DE VRIES, P.C., PARK, H.K., MUNSAT, T., GARCÍA-MUÑOZ, M. & SCHNEIDER, P.A. 2010 2D electron cyclotron emission imaging at ASDEX Upgrade (invited). *Rev. Sci. Instrum.* **81** (10), 10D929.

GIMBLETT, C.G. & HASTIE, R.J. 1994 Calculation of the post-crash state and 1 1/2 D simulation of sawtooth cycles. *Plasma Phys. Control. Fusion* **36** (9), 1439–1455.

HENDER, T., WESLEY, J., BIALEK, J., BONDESON, A., BOOZER, A., BUTTERY, R., GAROFALO, A., GOODMAN, T., GRANETZ, R., GRIBOV, Y., *et al.* 2007 MHD stability, operational limits and disruptions. *Nucl. Fusion* **47** (6), S128.

HU, B., BETTI, R. & MANICKAM, J. 2006 Kinetic stability of the internal kink mode in ITER. *Phys. Plasmas* **13** (11), 112505.

IGOCHINE, V., DUMBRAJS, O., ZOHM, H. & ASDEX UPGRADE TEAM 2008 Transition from quasiperiodicity to chaos just before sawtooth crash in the ASDEX Upgrade tokamak. *Nucl. Fusion* **48** (6), 062001.

IGOCHINE, V., DUMBRAJS, O., ZOHM, H., FLAWS, A. & ASDEX UPGRADE TEAM 2006 Stochastic sawtooth reconnection in ASDEX Upgrade. *Nucl. Fusion* **47** (1), 23.

IGOCHINE, V., *et al.* 2015 *Active Control of Magneto-Hydrodynamic Instabilities in Hot Plasmas*. Springer.

JARDIN, S.C., KREBS, I. & FERRARO, N. 2020 A new explanation of the sawtooth phenomena in tokamaks. *Phys. Plasma* **27** (3), 032509.

https://doi.org/10.1017/S0022377822000113 Published online by Cambridge University Press

KADOMTSEV, B.B. 1975 Disruptive instability in tokamaks. *Fiz. Plazmy* **1**, 710–715.

LICHTENBERG, A.J., ITOH, K., ITOH, S. -I. & FUKUYAMA, A. 1992 The role of stochasticity in sawtooth oscillations. *Nucl. Fusion* **32** (3), 495–512.

LUDA, T., ANGIONI, C., DUNNE, M.G., FABLE, E., KALLENBACH, A., BONANOMI, N., SCHNEIDER, P.A., SICCINIO, M., TARDINI, G., THE ASDEX UPGRADE TEAM & THE EUROFUSION MST1 TEAM 2020 Integrated modeling of ASDEX Upgrade plasmas combining core, pedestal and scrape-off layer physics. *Nucl. Fusion* **60** (3), 036023.

MUNSAT, T., PARK, H., CLASSEN, I., DOMIER, C., DONNÉ, A., LUHMANN, N., MAZZUCATO, E., VAN DE POL, M. & THE TEXTOR TEAM 2007 Localization of the magnetic reconnection zone during sawtooth crashes in tokamak plasmas. *Nucl. Fusion* **47** (11), L31–L35.

NAGAYAMA, Y., YAMADA, M., PARK, W., FREDRICKSON, E.D., JANOS, A.C., MCGUIRE, K.M. & TAYLOR, G. 1996 Tomography of full sawtooth crashes on the tokamak fusion test reactor. *Phys. Plasmas* **3** (5), 1647–1655.

NAVE, M.F.F., *et al.* 2003 Role of sawtooth in avoiding impurity accumulation and maintaining good confinement in JET radiative mantle discharges. *Nucl. Fusion* **43** (10), 1204–1213.

NISHIMURA, Y., CALLEN, J.D. & HEGNA, C.C. 1999 Onset of high-n ballooning modes during tokamak sawtooth crashes. *Phys. Plasma* **6** (12), 4685–4692.

PARK, H.K. 2019 Newly uncovered physics of MHD instabilities using 2-D electron cyclotron emission imaging system in toroidal plasmas. *Adv. Phys.:* X **4** (1), 1633956. Taylor & Francis. https://doi.org/10.1080/23746149.2019.1633956.

PARK, W., FREDRICKSON, E.D., JANOS, A., MANICKAM, J. & TANG, W.M. 1995 High-β disruption in tokamaks. *Phys. Rev. Lett.* **75** (9), 1763–1766.

PARK, W., PARKER, S., BIGLARI, H., CHANCE, M., CHEN, L., CHENG, C.Z., HAHM, T.S., LEE, W.W., KULSRUD, R., MONTICELLO, D., SUGIYAMA, L. & WHITE, R. 1992 Three-dimensional hybrid gyrokinetic-magnetohydrodynamics simulation. *Phys. Fluids* B **4** (7), 2033–2037.

SCHAFER, R.W. 2011 What is a Savitzky–Golay filter? [Lecture Notes]. *IEEE Signal Process. Mag.* **28** (4), 111–117.

SCIPY-NDIMAGE 2020 SciPy ndimage: Gaussian filter library. Accessed 25 March 2021. Available at: https://docs.scipy.org/doc/scipy/reference/generated/scipy.ndimage.gaussian_filter.html.

SPITZER, L. & HÄRM, R. 1953 Transport phenomena in a completely ionized gas. *Phys. Rev.* **89** (5), 977–981.

STEGMEIR, A., COSTER, D., MAJ, O., HALLATSCHEK, K. & LACKNER, K. 2016 The field line map approach for simulations of magnetically confined plasmas. *Comput. Phys. Commun.* **198**, 139–153.

STEGMEIR, A., COSTER, D., ROSS, A., MAJ, O., LACKNER, K. & POLI, E. 2018 GRILLIX: a 3D turbulence code based on the flux-coordinate independent approach. *Plasma Phys. Control. Fusion* **60** (3), 035005.

TOBIAS, B., KONG, X., LIANG, T., SPEAR, A., DOMIER, C.W., LUHMANN, N.C., CLASSEN, I.G.J., BOOM, J.E., VAN DE POL, M.J., JASPERS, R., DONNÉ, A.J.H., PARK, H.K. & MUNSAT, T. 2009 Advancements in electron cyclotron emission imaging demonstrated by the TEXTOR ECEI diagnostic Upgrade. *Rev. Sci. Instrum.* **80** (9), 093502.

VEZINET, D., IGOCHINE, V., WEILAND, M., YU, Q., GUDE, A., MESHCHERIAKOV, D., SERTOLI, M., THE ASDEX UPGRADE TEAM & THE EUROFUSION MST1 TEAM 2016 Non-monotonic growth rates of sawtooth precursors evidenced with a new method on ASDEX Upgrade. *Nucl. Fusion* **56** (8), 086001.

WESSON, J. & CAMPBELL, D.J. 2011 *Tokamaks*, vol. 149. Oxford University Press.

YAMADA, M., KULSRUD, R. & JI, H. 2010 Magnetic reconnection. *Rev. Mod. Phys.* **82** (1), 603–664.

YU, Q., GÜNTER, S. & LACKNER, K. 2015 Numerical modelling of sawtooth crash using two-fluid equations. *Nucl. Fusion* **55** (11), 113008.

ZOHM, H. 2015 *Magnetohydrodynamic Stability of Tokamaks*. John Wiley & Sons.